Computers in Biology and Medicine 180 (2024) 108938

Contents lists available at ScienceDirect

Computers in Biology and Medicine

journal homepage: www.elsevier.com/locate/compbiomed

Torque expression of superelastic NiTi V-Slot and conventional stainless steel orthodontic bracket-archwire combinations - A finite element analysis

Thomas Stocker, Andrea Wichelhaus, Uwe Baumert, Mila Janjic Rankovic, Corinna Lesley Seidel, Hisham Sabbagh *

Department of Orthodontics and Dentofacial Orthopedics, LMU University Hospital, LMU Munich, Goethestraße 70, 80336, Munich, Germany

ABSTRACT

Background: To investigate the torque expression of conventional stainless steel (SS) brackets in combination with rectangular SS archwires and nickel-titanium (NiTi) V-slot brackets in combination with V-shaped NiTi archwires using finite element analysis (FEA).
Methods: CAD models were created for a conventional bracket and rectangular archwires with dimensions of 0.018″x0.025″ and 0.019″x0.025″, and for a V-slot bracket and V-shaped archwires with heights of 0.55 mm, 0.60 mm and 0.70 mm. FEA was performed using Ansys 2022R2 software to assess the forces and moments during simulated torsion of the archwires in the brackets between 0° and 25° with varying interbracket distances and free path lengths.
Results: The V-slot bracket-archwire combination exhibited force transmission and moment generation within 1° of torsion. The transmissible force increased with the torsion angle, but showed an upper limit of about 13–14 Nmm. The SS bracket-archwire combination showed negligible forces and moments for simulated torsion between 0° and 15°. At torsions of 25°, moments of 12 Nmm and 14 Nmm occurred for the 0.018″x0.025″ and 0.019″x0.025″ archwire dimensions, respectively.
Conclusions: The V-slot bracket-archwire combination is effective in expressing torque and preventing both over- and under-activation. Conventional bracket-archwire combinations showed torsional losses due to play between 10 and 15°, depending on the dimensions of the respective archwire, and no upper torsional moment limit.

1. Introduction

In orthodontic therapy, correction of labiolingual inclination of both posterior and anterior teeth is considered essential to achieve stable static and dynamic occlusal relationships and physiological overjet [1]. Biomechanically, in order to achieve a therapeutic change in the labiolingual inclination of the teeth, a torsional moment is required [2]. Fixed orthodontic multibracket appliances are most suitable to perform such tooth movements by the interaction between the archwire and the bracket, which is usually referred to as torque transmission [3,4]. The torque results from the inclination of the bracket slot in relation to the archwire, whereby the twisted archwire generates the necessary moments through its restoring force when inserted into the bracket [5].

In the edgewise technique, to correct labiolingual inclination, torque was applied by twisting the orthodontic archwire for the individual teeth, which is difficult to control and time-consuming. The subsequent introduction of the straight-wire technique aimed to minimize archwire bends, by taking into account the desired final teeth positions and integrating the first-, second- and third-order information in the geometry of the brackets (prescription) [6]. In theory, preadjusting the appliance should induce the necessary force system for an idealized tooth position. While in-out (orovestibular position) and tip (mesio-distal inclination) characteristics show adequate to full expression, torque expression in the straight-wire technique remains limited and individual bends or prefabricated partially twisted archwires are still required [1,7–9]. This phenomenon is mainly attributed to the torsional play between the archwire and the bracket slot, as this can introduce a significant inaccuracy in force transmission [7,10,11]. Torsional play between the bracket and archwire is inherent in most bracket systems due to their design [12,13] and is even required in some phases of treatment to reduce friction during translational tooth movements [14]. Orthodontic archwires have varying torsional play in the slot, depending on its dimensions. The theoretical torsional play of a 0.019″ × 0.025″ archwire in a 0.022″ wide slot equals nominally 7° [13]. However, the effective torsional play has been found to be larger than published theoretical values, ranging from 15° to 35° for the same dimensions, depending on the manufacturer and bracket/archwire combination [5,15]. These deviations may be due to dimensional manufacturing tolerances for wire height and width as well as inaccuracies in edge rounding of orthodontic archwires and finally also deviations in the width of the bracket slot. Depending on the treatment step and bracket system, this can reduce the effective torsional moment and thus clinical tooth

* Corresponding author.
E-mail address: hisham.sabbagh@med.uni-muenchen.de (H. Sabbagh).

https://doi.org/10.1016/j.compbiomed.2024.108938
Received 12 October 2023; Received in revised form 18 June 2024; Accepted 22 July 2024
Available online 30 July 2024

movement to negligible values, resulting in underactivation. Manual application of individual twist bends to overcome torsional play can result in overactivation and potentially root resorption due to the high Young's modulus and thus small activation range of stainless steel archwires [1].

Several developments have been introduced in recent years to overcome limitations of fixed orthodontic straight-wire appliances. These include, among others, individualized CAD/CAM (computer-aided-design/computer-aided-manufacturing) bracket systems or indirect bonding trays for bracket positioning [17,18]. Both measures are aimed at controlling the force and moment systems acting on the brackets more precisely. Despite the great effort required to manufacture and position these brackets, hardly any improvements in efficiency have been observed [19] and the inclination of anterior teeth still deviate from the virtual treatment simulation [16,17].

Another approach to reduce the influence of torsional play is to change the bracket and archwire designs and thus their interaction mechanism. A special design of the linear guide, a triangular or dovetail guide, was proposed for a newly developed bracket with regard to the slot shape [10]. It has the advantage of being intrinsically free of play and its design allows high precision in guiding tasks, potentially overcoming a key limitation of current straight-wire bracket systems. To integrate this guiding principle, both the bracket and the archwire were redesigned to adopt a trapezoidal or V-shape. Furthermore, the newly developed bracket is made entirely from a superelastic nickel-titanium (NiTi) alloy, in contrast to most brackets today, which are usually made from stainless steels, polycrystalline aluminium oxide, zirconium dioxide or plastic [20,21]. In contrast to steels, NiTi alloys exhibit relatively low Young's moduli at the beginning of loading and then form a stress plateau, which offers a high reversible strain of up to 8 %. This allows the bracket to respond elastically to loads over long distances. The suitability of the new superelastic orthodontic bracket and V-shape bracket-archwire concept for efficient generation of torsional moment has already been demonstrated [10].

However, the detailed process of bracket-archwire interaction during torsional moment transmission of the superelastic in comparison to conventional bracket systems has not been investigated to date. Since the tooth movements can be classified as quasi-static, a comprehensive analysis of bracket and archwire deformations and moment generation is not feasible in vivo. In contrast, finite element analysis (FEA) allows the investigation of mechanical behavior of orthodontic appliances in silico and derivation of clinical results, at least to a certain degree of accuracy [2,22].

Aim of this study was to analyze the torque expression comparing superelastic NiTi V-Slot and conventional stainless steel orthodontic bracket-archwire combinations using finite element simulations.

2. Material & methods

Since the transmission of torsional moment in the slot depends on various variables, a variation of the main system variables, the inter-bracket distance, the material of the bracket, the material of the archwire, the type of bracket and the rotation of the archwire itself was performed to be able to describe and compare the systems.

For the FEA, the model of a V-slot bracket and the complementary V-archwire were converted into CAD models according to a template provided by the manufacturer (redsystem GmbH, Munich, Germany). Autodesk Inventor 2021 (Autodesk, Inc., San Rafael, CA, USA) was used to design the models (Figs. 1 and 2). The dimensions of the initial archwire were chosen to achieve a cross-sectional area similar to that of a conventional 0.017″ × 0.025″ archwire. Furthermore, additional two V-shaped archwire types with different heights and therefore different cross-sectional areas were included into the simulations. Accordingly, the slot size of the V-slot bracket corresponds to the archwire size (Fig. 1). Beside that, different interbracket distances or free path lengths were chosen for the analysis of the V-archwire.

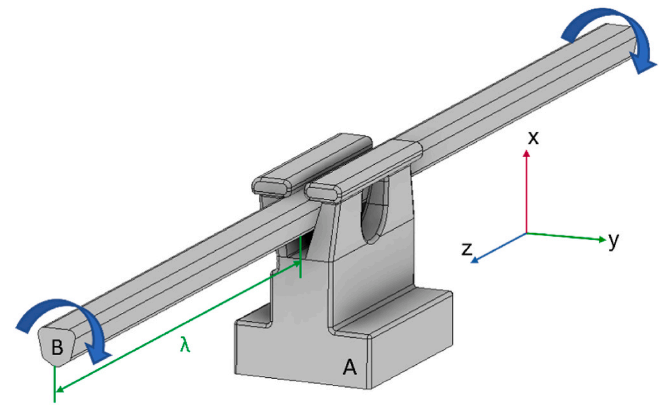

Fig. 1. Model of the V-wire (B) and the V-slot bracket (A). The blue arrows show the direction of the rotation applied in the finite element simulations. The green arrow shows the free path length λ.

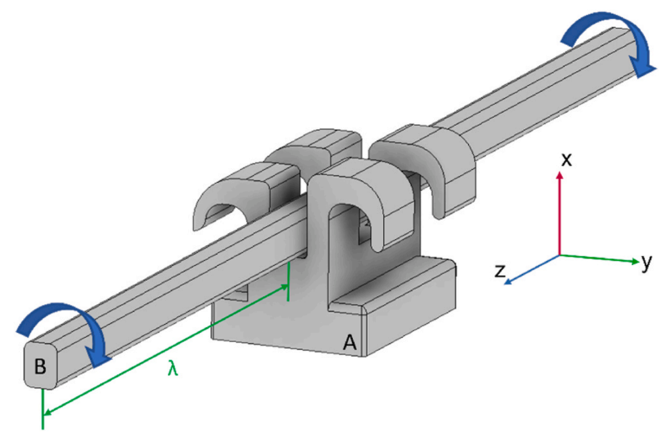

Fig. 2. Model of rectangular archwire (B) with dimensions 0.019″ × 0.025″ and conventional twin bracket with slot width of 0.022" (A). The blue arrows show the direction of the rotation applied in the finite element simulations. The green arrow shows the free path length λ.

Furthermore, a model of a twin bracket with a slot size of 0.022″ and rectangular archwires of dimensions 0.018″ × 0.025″ and 0.019″ × 0.025" (Fig. 2) were created. An edge rounding with a radius of 0.1 mm was included in all archwire models. To achieve a common orientation a coordinate system was established. The x-axis was defined perpendicular to the bottom of the slot, the y-axis pointed to the occlusal wing of each bracket and the z-axis was parallel to the slot or the long side of the archwire, respectively (Figs. 1 and 2).

The archwires and brackets were combined into an assembled model in Inventor 2021 via inserted geometric constraints and subsequently imported into Ansys 2022R2 (Ansys, Inc., Canonsburg, PA, USA). The integrated meshing tool was used to mesh the models. Appropriate SOLID 186 and SOLID 187 elements were automatically generated. The mesh density was chosen to be finer at the parts of the superelastic NiTi brackets, particularly the flexure hinge of the gingival wing, due to its comparatively delicate geometry, to accurately capture the detailed stress distribution and minimize errors due to stress gradients and ensure robust simulation results. Material parameters for the twin brackets (17-4 PH steel/X5CrNiCuNb16-4) and for the rectangular archwires (316 steel/X5CrNiMo17-12-2) were chosen from the Ansys internal database. For the NiTi V-slot bracket, as well as the V-shaped archwire, the NiTi model from Ansys was applied using the set of parameters outlined in Table 1. Frictional contacts were chosen to simulate application-related archwire motion, using the pure-penalty detection method and an unsymmetric Newton-Raphson algorithm to achieve

Table 1

Material parameters for the FE material model for NiTi alloys in Ansys. The parameters for steel materials at 20 °C were already integrated in Ansys. For the sake of completeness their parameters for $\vartheta = 36$ °C are listed here. The values of the "break-off" stress points on the curve are derived from literature and own measurements [23].

Parameter	NiTi M1 Value	Steel 17-4 PH	Steel 316
Young's-modulus E	70 GPa	204 GPa	195 GPa
Poisson's ratio ν	0.33	0.291	0.25
σ_{SAS}	400 MPa	–	–
σ_{FAS}	480 MPa	–	–
σ_{SSA}	250 MPa	–	–
σ_{FSA}	160 MPa	–	–
ϵ	0.063	–	–
α	0	–	–

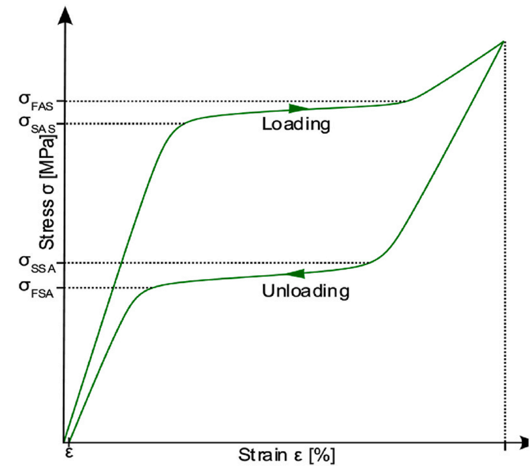

convergence. The corresponding frictional coefficients of $\mu = 0.25$ for NiTi-NiTi contacts and $\mu = 0{,}15$ for steel-steel pairs were applied. The frictional coefficients were selected from literature and resemble material pairings with saliva as the interfacial medium, reflecting the situation in the mouth where the bracket is constantly immersed in saliva (Kusy et al., 1998). Contact trimming was deactivated so that the contact could be found reliably. The material behaviour was calculated using the constitutive equations integrated in Ansys.

The number of nodes and elements of the mesh for each model are listed in Table 2. Due to the nonlinearities resulting from the contact calculations, the load was divided into several loading steps. The exact number of sub-load steps is automatically set by the FE software Ansys to achieve a converging solution. Each load steps amounted to a maximum of one hundredth of the applied torsion, resulting in minimum 20 and maximum of 1000 substeps.

The boundary conditions were selected as follows: A fixed support was applied to the base of the brackets. To avoid rigid body movement, the archwires were constrained against longitudinal motion via a remote displacement of zero. Also, a rotation around the axis normal to the longitudinal axis of the archwire and parallel to the bracket-slot was constrained by a remote displacement of zero. Further movements were prevented by automatic integration of weak springs. Due to the nonlinearities regarding the NiTi material properties, as well as the nonlinearities originating from the contact calculations, the "large deformations" option was activated. A thermal condition of 36 °C ambient temperature was applied before deformation. For the deformation of the archwires, an external displacement was chosen at both ends of the archwire as a rotation between 5° and 25° (Figs. 1 and 2), depending on the bracket-archwire combination. In order to allow rotation of the archwire, all degrees of freedom were chosen as free, except the z-axis and the rotation around y-axis.

In order to classify the play existing between the bracket and the archwire, the dimensions including edge rounding were measured for different commercially available archwires using a light band micrometer with a resolution of ±0.5 μm (Keyence LS900, Keyence Deutschland GmbH, Neu-Isenburg, Germany) and a Mahr micrometer screw gauge (Mahr GmbH, Goettingen, Germany) (Fig. 3).

From the dimensions, the effective diagonal dimension could be calculated according to DIN 13996. Subsequently, it was possible to calculate the respective play of the archwires in the slot and the corresponding difference to "ideal" formed archwires using these values. For each wire type, twelve different samples were measured. These measurements were repeated four times each. From the four measurements an average value for each sample was calculated and from these averaged values again an average value was calculated for each wire type.

3. Results

The results of the FEA are combined within the following tables. They are divided by the free path length λ of the archwires outside of the bracket and the height of the archwire itself. In Table 3 the results of the torsion for an archwire with free path length of $\lambda = 3.0$ mm, $\lambda = 8.0$ mm

Table 2

Number of elements, nodes, and element sizes used in the FE simulation for the bracket and respective archwire models (λ = interbracket distance or free path length).

Bracket	Archwire Geometry	Dimension	Element size [mm]		Elements	Nodes
			Bracket	Archwire		
Twin (0,022“ Slot)	Rectangular ($\lambda = 13$ mm)	0.018“ x 0.025“	0.4	0.07	191,893	391,698
		0.019“ x 0.025“	0.4	0.07	170,332	362,342
V-Slot	V-shape ($\lambda = 3$ mm)	h = 0.55 mm	0.2	0.1	169,663	288,185
		h = 0.6 mm	0.2	0.1	170,249	289,698
		h = 0.7 mm	0.2	0.1	173,600	296,328
	V-shape ($\lambda = 8$ mm)	h = 0.55 mm	0.2	0.1	126,705	217,953
		h = 0.6 mm	0.2	0.1	164,440	260,916
		h = 0.7 mm	0.2	0.1	172,618	329,578
	V-shape ($\lambda = 13$ mm)	h = 0.55 mm	0.2	0.1	123,740	230,179
		h = 0.6 mm	0.2	0.1	168,184	276,982
		h = 0.7 mm	0.2	0.1	176,632	301,210

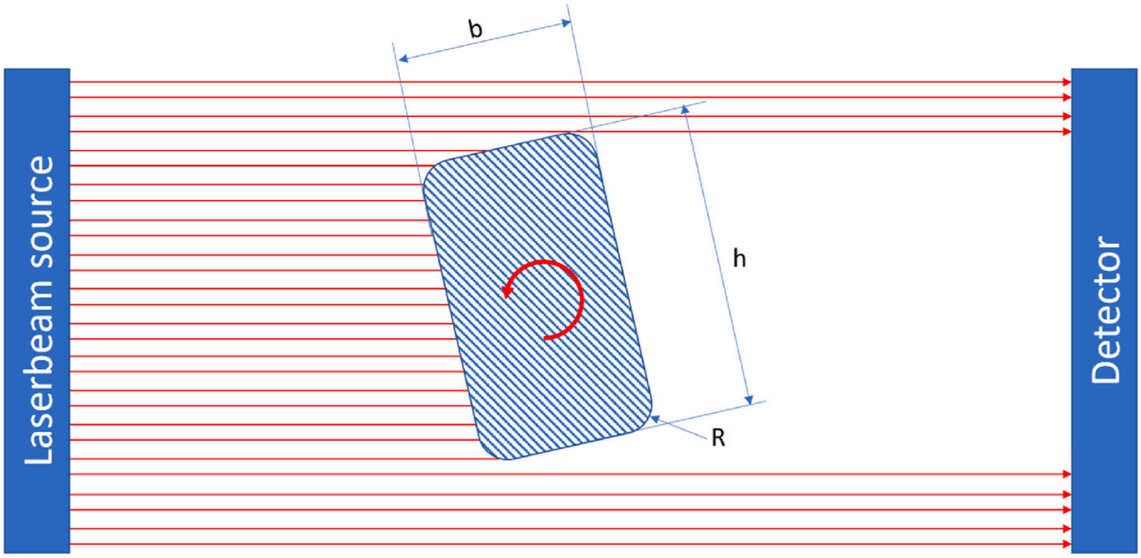

Fig. 3. Graphical representation of the measurement method for the commercially available 0.018″ × 0.025″ and 0.019" × 0.025″ arcs with the light band micrometeter. The sections of the archwire to be measured are indicated by b (edgewise), h (ribbonwise) and R (archwire edge rounding).

Table 3
Calculated forces at the occlusal and the gingival wing of the V-slot Bracket in combination with a V-formed archwire, as well as the resulting maximum moments at the base of the bracket and 0.3 mm below the slot floor as a function of the torsional angle and the archwire's height with a free path length of λ = 3.0 mm, λ = 8.0 mm and λ = 13.0 mm.

Height [mm]	Torsion angle [°]	Force @ wing [N]			Torsional moment [Nmm]		
		λ = 3 mm	λ = 8 mm	λ = 13 mm	λ = 3 mm	λ = 8 mm	λ = 13 mm
0.55	5	2.05	1.29	0.99	0.91	0.58	0.45
	10	13.30	8.02	5.69	5.52	3.46	2.47
	15	18.40	15.19	11.05	6.88	6.24	4.68
	20	18.36	18.43	16.30	6.89	7.10	6.60
0.60	5	3.97	2.38	1.70	1.98	1.19	0.86
	10	17.77	10.51	7.22	8.31	5.11	3.59
	15	20.14	18.68	13.25	9.13	8.55	6.32
	20	20.28	20.27	19.32	9.08	8.89	8.57
0.70	5	8.50	4.22	2.88	5.14	2.57	1.75
	10	25.62	13.78	9.19	13.94	8.23	5.55
	15	28.08	23.70	15.70	13.92	13.37	9.31
	20	30.58	28.71	22.38	13.95	13.91	12.95

and λ = 13.0 mm and three different heights are listed. In detail the maximum forces at the occlusal wing and the maximum moments directly at the bracket's base and at a distance d = −0.3 mm underneath the bracket slot, which corresponds to the tooth crown surface, are shown.

Forces and moments were already generated at a torsion angle of 5°, with F = 2.05 N and M = 0.91 Nmm for a height of h = 0.55 mm. Furthermore, the occurring forces and moments increased with increasing torsion angle independent of the height of the archwire. The highest force value at the occlusal wing at a torsion of 20° was exhibited by the archwire with a height of h = 0.70 mm (F = 30.58 N). It is noticeable that the increase of the torsional angle did not cause a uniform increase of the forces and moments. For example, the force values increased by more than 13 N between 5° and 10°, but only by about ΔF≈2.5 N between 10° and 15° for a height of h = 0.60 mm. Within the next interval, the increase in force values was less than 0.2 N. For the moments, an increase of ΔM≈6 Nmm applied between 5° and 10° torsion and again less than ΔM≈1 Nmm between 10° and 15°. It is clearly visible that the maximal transmitted torsional moment rises from M = 6.89 Nmm for h = 0.55 mm, to M = 9.08 Nmm for h = 0.60 mm, to finally M = 13.95 Nmm for h = 0.70 mm.

The results with λ = 8 mm (cf. Table 3) show that the initial values at a torsion of 5° were lower than with the smaller free path length. The highest force at the occlusal wing for 5° torsion was exhibited by the h = 0.70 mm archwire with F = 4.22 N. The highest moment below the slot at a torsion of 5° was obtained with an archwire height of h = 0.70 mm with M = 2.57 Nmm, whereas h = 0.55 mm provided only M = 0.58 Nmm. Again, the results for the largest torsion angle of 20° showed the highest resulting forces and torsional moments. Thus, a force on the occlusal wing of F = 18.43 N was calculated for h = 0.55 mm up to F = 28.71 N for h = 0.70 mm. Similarly, the highest resulting torsional moments below the slot were obtained at the highest torsion; for h = 0.55 mm M = 7.10 Nmm was calculated, then at h = 0.60 mm M = 8.89 Nmm and finally for h = 0.70 mm M = 13.91 Nmm. Furthermore, the forces and moments increased between 5° and 10° torsion by ΔF≈ 6.7 N and ΔM≈ 2.9 Nmm, respectively. Between 10° and 15° torsion, similar values resulted with ΔF≈ 7.2 N and ΔM≈ 2.8 Nmm, respectively. For the jump between 15° and 20° torsion, the differences decreased to ΔF≈ 3.2 N and ΔM≈ 0.9 Nmm, respectively, for a height of h = 0.55 mm. Similar to this the increase for a height of h = 0.7 mm between 5° and 10° torsion is ΔF≈ 9.6 N and ΔM≈ 5.7 Nmm, respectively. For the interval between 10° and 15° torsion, ΔF≈ 9.9 N and ΔM≈ 5.1 Nmm, respectively, were calculated. Between 15° and 20° torsion the force and moment increase amounted to ΔF≈ 5.0 N and ΔM≈ 0.50 Nmm.

Lastly, FEA was performed with λ = 13 mm (cf. Table 3). Here, again lower forces and torsional moments were seen at the lowest torsion of 5°. It is clearly visible that the resulting forces and moments increase with increasing torsional angle and increasing archwire height. The strongest torsion of 20° again evoked the highest forces and moments. These amounted to approx. F = 16.30 N for h = 0.55 mm, F = 19.32 N for h = 0.60 mm and F = 22.38 N for h = 0.70 mm. Torsional moments below the slot bottom ranged from M = 6.60 Nmm for h = 0.55 mm to M = 12.95 Nmm for h = 0,70 mm. Similar to the FE analyses before the difference in force and torsional moment generation decreased with increasing torsional angles. The change in the resulting torsional moments or forces, were ΔM≈ 2–3.8 Nmm and ΔF≈4.7–6.3 N for the interval between 5° and 10° torsion. Increasing the torsion from 10° to 15° resulted in differences of ΔF≈2.2–5.4 N and ΔM≈3.8–6.5 Nmm.

As shown in Fig. 4, the generated torsional moment increases with increasing torsional angle. For longer free path lengths the maximum torsional moment is reached later than for shorter free path lengths.

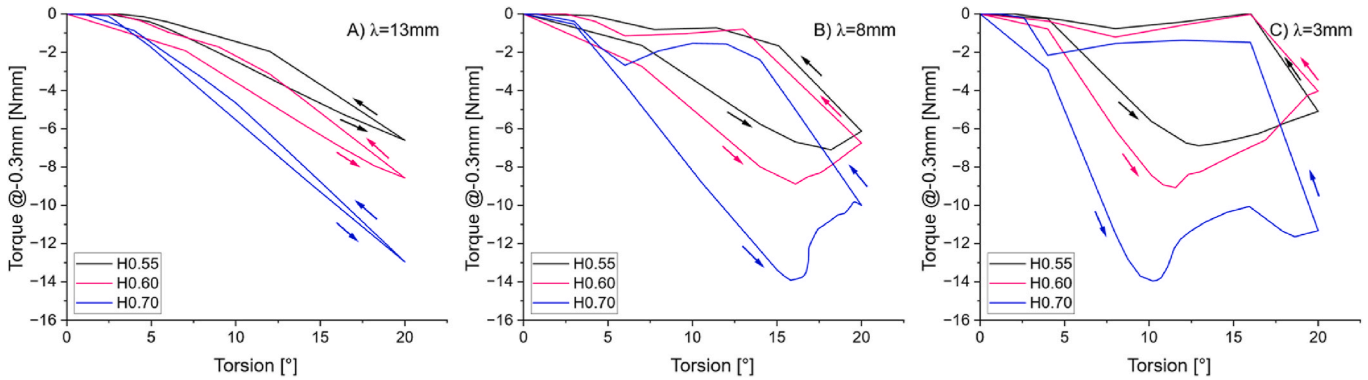

Fig. 4. Calculated torsional moment generated at 0.3 mm underneath the slot bottom (=tooth crown surface) plotted against the torsional angle and separated according to the respective free path length λ. The phase of the load is represented by the lower path in each case. The relief, on the other hand, is represented by the higher path. The direction of the progression is indicated by colored arrows, corresponding to the color of the curve. It can be concluded, that with higher free path length the maximum torsional moment is reached at lower angles. However, the course of the torsion-torsional moment curve becomes more distorted.

However, the shorter the free path length, the more distorted the curve gets after the maximum torsional moment was reached. This maximum torsional moment lies between 12.95 Nmm and 13.95 Nmm (cf. Table 3) for the highest archwire height $h = 0.7$ mm depending on the exact configuration. The maximum for $h = 0.6$ mm is within the interval from 8.57 Nmm to 9.07 Nmm and for $h = 0.55$ mm between 6.60 Nmm and 7.10 Nmm. To show the differences in mechanical response or deformation under load between the V-slot and conventional bracket, comparative von-Mises stresses from the FEA are presented in Fig. 5.

The simulations of the torsion of the rectangular SS archwires with dimensions 0.018″ × 0.025″ and 0.019″ × 0.025″ in a rectangular SS slot and a free path length of $\lambda = 13$ mm led to the results in Table 4. The play for an archwire of dimension 0.018″ × 0.025″ were be calculated to $\gamma \approx 14.64°$ and for an archwire of dimension 0.019″ × 0.025″ to $\gamma \approx 10.75°$. Therefore, simulation of torsion below these angles was not performed. Torsion of a 0.018″ × 0.025″ archwire by 15° resulted in negligible force and moment values in the simulation. As already observed for the V-archwires, the resulting moments and forces increase with the increase of torsion. Also, the difference of the generated forces and moments between the intervals of the torsional angle differences are getting lower with increasing angles.

From the measurements of the different wire dimensions, as shown in 5, as well as it is clearly visible that all commercially available archwires measured did not exhibit the stated norm dimensions. Indeed, almost all wire types have smaller dimensions than intended. This also leads to smaller play angles than theoretically calculated.

Table 4
Results of FE simulations for torsion of rectangular arches in rectangular slots divided by arch dimension and torsion of the arch. The results are the forces on the wings, as well as the resulting moments at the base and 0.3 mm below the slot and $\lambda = 13$ mm.

Dimension [inch]	Torsion angle [°]	Force @ wings [N]	Torsional moment [Nmm]
0,018″ x 0,025″	5	0	0
	10	0	0
	15	$5.88 \bullet 10^{-6}$	$1.62 \bullet 10^{-3}$
	20	20.03	8.29
	25	29.79	12.28
0,019″ x 0,025″	5	0	0
	10	0	0
	15	16.30	7.10
	20	30.50	13.23
	25	32.46	14.06

4. Discussion

This study investigated the torque expression in conventional

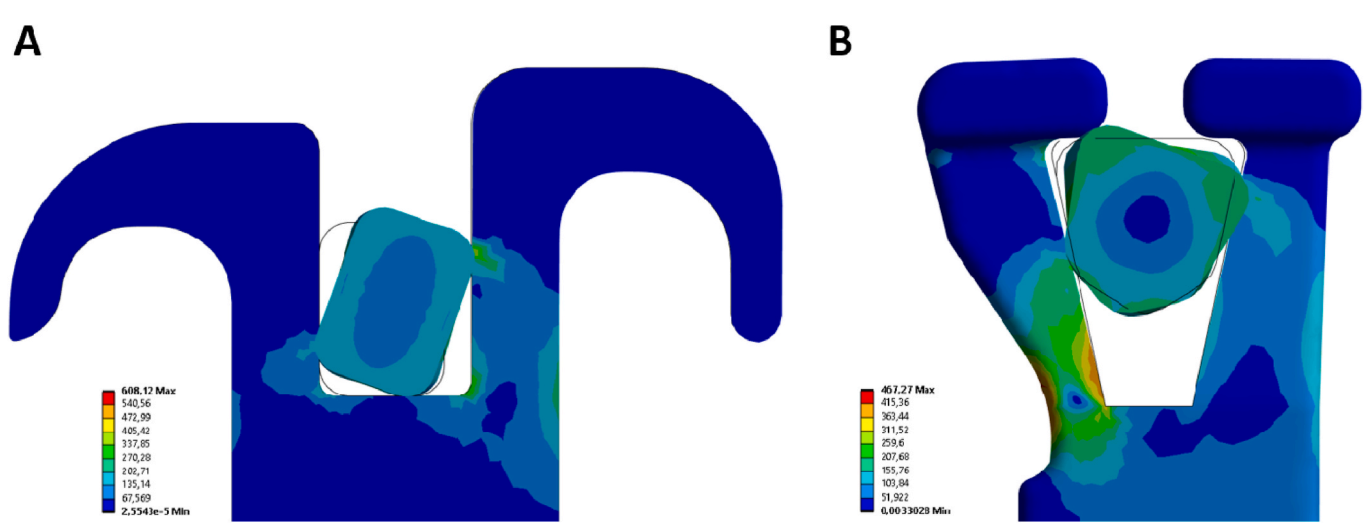

Fig. 5. Comparison of the mechanical response of a conventional stainless-steel bracket and a 0.018" x 0.025″ archwire (A) with a superelastic NiTi V-slot bracket (B) and a 0.55 mm height archwire under torsional loading. The colored models show the final state at maximum torsion of the arch wire; the black lines, on the other hand, show the respective undeformed initial models. The heatmap displays the von-Mises stresses in MPa.

stainless-steel brackets with rectangular archwires and superelastic NiTi V-slot brackets with V-shaped archwires using finite element simulations.

The generation of suitable moments through torque expression in fixed orthodontic therapy is essential for the labiolingual alignment of teeth. If the generated moments are too small, the efficiency of tooth movement is limited, whereas if the moments are too large, there is a risk of apical root resorption [1]. In the straight-wire technique, torque expression is limited, primarily due to torque play between bracket and archwire, requiring pretorqued archwires or twist bends that can be difficult to control. In contrast, the V-slot bracket is designed to be practically free of play when using a complementary V-shaped archwire [10]. The findings of the present FEA with regard to the torsional play and the resulting moments are in line with a previous biomechanical study, which, however, investigated only one V-archwire dimension and constant free path lengths for all archwires [10].

When investigating torqueing effects, the length of the wire outside the bracket slot λ ("free path length") must be taken into account. This applies to both V-slot nickel-titanium brackets as well as stainless-steel brackets with a rectangular slot. As known from simple mechanics for an archwire clamped on one side, less torsional moment is generated as the free path length increases. This behavior follows the equation for the torsional moment M_t [24]:

$$M_t = \frac{(\phi \bullet G \bullet I_t)}{\lambda}$$

With ϕ = torsion angle, G = shear modulus, I_t = torsional moment of inertia, λ = free path length.

However, this equation only shows the behavior that would be exhibited by an archwire that is clamped immovably in the bracket, for example by means of a ligature wire or a clip of an active self-ligating bracket. Clinically, the archwire has to have play in the slot as the slot width must be bigger than the archwire's. Otherwise the assembly of the two components is impossible. This is especially necessary if torsional moment should be applied. In this case an archwire has to fit in the slot even if it is twisted around its longitudinal axis. As long as the play isn't fully consumed by the twisting of the archwire, no torsional moment can be produced. The equation above therefore is only applicable from the depletion point of the play. Nevertheless, with shorter free path lengths, the limit value of the torsional moment generated in the bracket will be reached at lower torsion angles than with larger free path lengths (Fig. 6). For this reason, it is necessary to report information on the free path length if FEA, in vitro or in vivo experiments are conducted. Without this information the generated torsional moment values cannot be compared properly. This may be especially true for highly idealized calculations like finite element simulations, as side effects are almost completely excluded.

The results of the finite element simulations for the V-slot bracket showed that the force transmission from the archwire to the wings already takes place at very low torsion angles below 1° and moments are generated almost from the beginning of the torsional movement (cf. Fig. 4). The transmissible force increases with an increase of the torsion angle, but is limited by the geometry of the V-shaped archwire in interaction with the flexibility based on the superelasticity of the bracket wings. As can be seen from Fig. 4 it becomes clear that the moment approaches an upper limit depending on the chosen height and free path length of the archwire.

The upper limitation of the magnitude of the generated torsional moments is firstly due to the resulting stress plateau of superelastic NiTi archwires. With reference to the above equation, the influence of material and shape is particularly visible in the torsional stiffness S_t=G• I_t. It consists of the shear modulus and the torsional moment of inertia. Furthermore, the interaction between the archwire's geometry and the elastic deformability of the wings accounts for this upper limit of the possible torsional moments. If the archwire is twisted in the slot, the diagonal of the archwire approaches finally a horizontal line. This in turn causes a reduction in the effective lever arm acting on the limiting

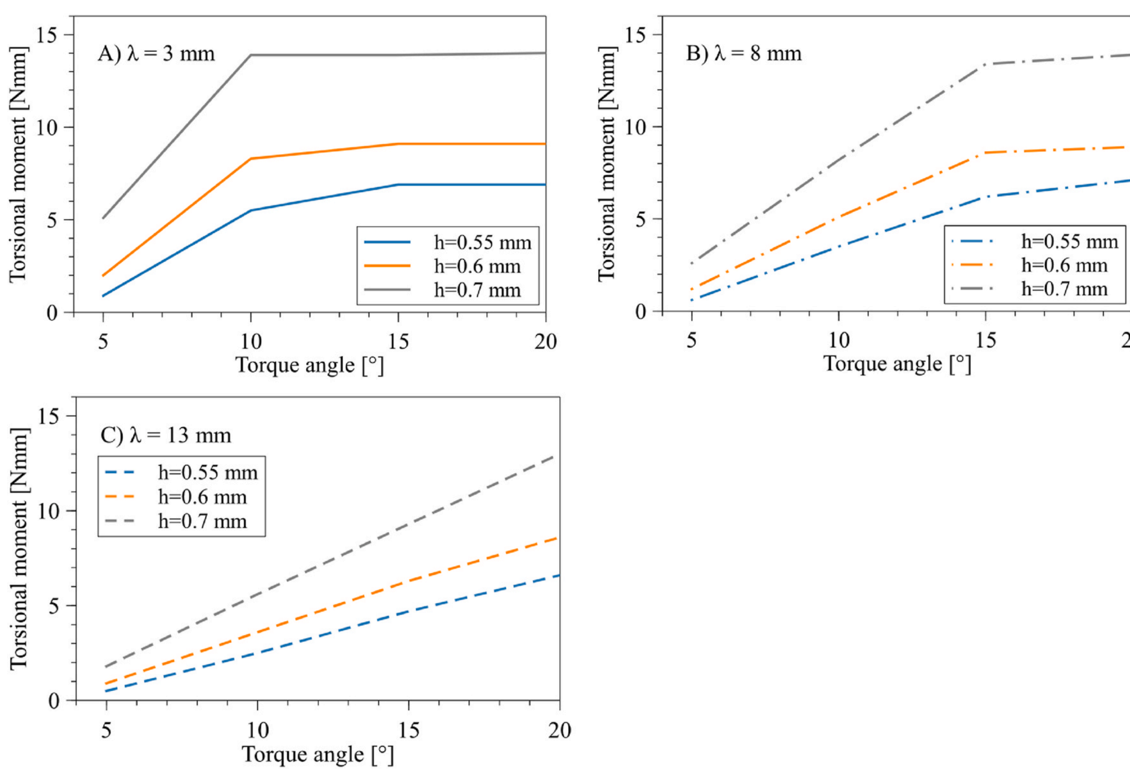

Fig. 6. Comparison of the influence of the free path length λ on the resulting torsional moment in dependence of the torque angle for the V-slot bracket-archwire combination. It is clearly visible that lower free path lengths cause higher torsional moments at the same torque angles. Additionally, the torsional moment limit is reached earlier for the lower free path lengths.

wings, due to the deformability of the wings, which can diverge under load. By increasing the height h of the archwire, the effective lever arm and thus the resulting torsional moment is increased. Despite the increase in the transmitted forces and generated torsional moment values the archwire will finally deform the elastic wings of the NiTi bracket and not be able to generate higher torsional moment values. This upper limit of the torsional moment was found to be around 13–14 Nmm, (Tables 1–3), which is well within the range where tooth movement occurs, which is recommended to be between 5 and 20 Nmm [13,25,26]. There is a tendency for smaller torsional moments to be advantageous, as they are expected to have less pronounced side effects, such as root resorption [27].

For the conventional stainless-steel bracket, the finite element simulations of the rotation of rectangular archwires in the rectangular slot showed significant losses of rotational angles due to play between archwire and bracket. This means that force transmission is only possible at larger torsion angles from approx. 10°–15°, depending on the dimensions of the respective archwire. The loss of torsional angle and accordingly of transmissible torsional moment in conventional bracket-archwire combinations is therefore 10° and thus up to one third of the specified torque angle value. However, these maximum angles are only valid if the archwire has direct contact to one wall of the slot, which introduces an additional degree of uncertainty into the transfer of torsional moment. Therefore, it is necessary to first compensate the play of the archwire in the slot by torsion of the archwire. Also, the amount of play can only be predicted within rough limits. Due to the high stiffness of the bracket wings, the maximum possible transmitted torsional moment is not limited as it is shown in the V-slot bracket, where the archwire is able to "spin" in the slot if the maximum torsional moment value is exceeded unintentionally. Thus, higher overall torsional moments can be applied when using rectangular archwires in the rectangular slot, although not always physiologically appropriate. However, since the exact amount of torsional moment acting cannot be accurately estimated due to the play, the practitioner must exercise caution when selecting archwires with torque, because there is no torsional moment limit built into the conventional in opposite to the V-slot bracket. This observation is particularly relevant as significant differences are observed between the nominal and actual dimensions of rectangular orthodontic archwires [5]. This can result in a significant discrepancy between the expected and actual torsional moments generated, which can lead to underactivation without clinical tooth movement or overactivation with periodontal overload and possibly orthodontically induced inflammatory root resorptions (OIIRR) [5,28].

In summary, the V-bracket-archwire combination offers two advantages that are conducive to effective force and moment transmission:

1. Due to the self-centering properties of the V-shaped orthodontic bracket-archwire combination, torque transmission was shown to be relatively independent of the torsion and dimension of the archwire. Torsional moments were generated already at very small torsion angles below 1°, irrespective of the simulated archwire height. As no torsional moment is lost due to archwire play in the slot, underactivation can be practically avoided. The required amount of torque could be obtained by using archwires of different heights. This could make it easier for the practitioner to apply the appropriate torsional moments clinically.
2. The amount of torsional moment is limited by the elasticity of the bracket, which prevents excessive force and moment transmission to the teeth. On the one hand, this limitation prevents overactivation, but on the other hand, it also prevents the use of intentionally high torsional moments. In order to be able to transmit higher moments, special clips ("caps") injection moulded from of polymers, such as polycarbonate (PC) or polyetheretherketone (PEEK), were designed to couple the wings mechanically. This prevents the archwire from spinning, and also from unintended deformation of the wings, thus enabling the expression of higher torsional moments as long as the cap is applied [29].

For both rectangular stainless steel bracket-wire combinations investigated, it should be noted that the actual dimensions of the bracket slot and wires influence the torque expression. It is possible to calculate a theoretical play angle, using dimensional parameters of the archwire, as described by the following equations [30]:

$$\gamma = \alpha - \beta = \sin^{-1}\frac{(S-2r)}{d} - \sin^{-1}\frac{(h-2r)}{d} \text{ and } d = \sqrt{(w-2r)^2 + (h-2r)^2}$$

Where d = diagonal of the wire to the centers of the corner radii; r = corner radius; w = width of the wire; h = height of the wire; γ = maximum angle of rotation of the wire from its vertical position; α = angle between the diagonal of the wire and the slot wall facing it; β = angle between the diagonal and the side of the wire facing it; S = width of the slot.

Despite this theoretical description of the possible play in the slot, the calculated values will only give an indication. As it became visible in the measurements, these values are never reached due to deviating effective dimensions of the arches. This, in return, results in an additional uncertainty in the estimation of the acting torsional moments. Furthermore, when considering the torsional moment transfer from the archwire to the slot, it must be considered that, for manufacturing reasons, archwires cannot have sharp edges but must have edge radii. As a result, the effective diagonal of the archwire, as shown in DIN 13996, is smaller than that calculated from the dimensions [31]. This can further increase the clearance in the slot and further decrease the realization of the desired rotation (Tepedino et al., 2020) and may not be observed if dovetail guide slots are used, because of the self-centering properties of this type of guide. This also applies to commercially available archwires, which are generally subject to manufacturing tolerances and do not comply with the specified theoretical dimensions.

As V-shaped archwires are a component under development, only a few prototypes were available at the time of the study, and solely virtual models were created for the simulations. However, due to the self-centering properties of the design, possible deviations in the dimension of the V-archwires should have negligible impact compared to rectangular archwires. Only very small play angles between the components were present irrespective of the simulated V-shaped archwire height. This behavior can be interpreted as limiting or restricting a degree of freedom of movement within the slot. Therefore, the wire is prevented from moving in occlusal-gingival directions, but still free to rotate or to move mesio-distally. Thus, for precise treatment, it is necessary to keep the sum of all rotation angle losses as small as possible. According to the results of this study, this can be achieved by the V-slot bracket with the complementary V-archwire. The required torsional moment can be accurately applied clinically by selecting the respective archwire dimension.

This study used FEA to investigate torque expression comparing two distinct orthodontic bracket designs, focusing on the bracket-archwire interaction. Several simulation parameters and boundary conditions were defined within the simulations. The boundary condition "fixed support" at the base of the bracket was used to simulate a rigid connection to the tooth. Any elasticity of the adhesive between the bracket and tooth was considered negligible. The marginal condition of archwire movement in the longitudinal direction was blocked, justified by the fact that the curved arch shape of the teeth clinically prevents longitudinal movements of the archwire due to tilting in neighboring brackets. Since the archwires should not tilt within the slot when correcting the tooth inclination, the rotation around the axis perpendicular to the longitudinal axis of the archwire and parallel to the bracket-slot was constrained by a remote displacement of zero. This was justified because the brackets are generally leveled before torque is applied clinically, making tilting unlikely in this setting. Other possible movements were reduced by the automatic integration of weak springs, which served primarily to stabilize the calculation.

Compared to the complex dynamics of clinical treatments involving a full archwire with different interbracket distances, multiple brackets-archwire interactions, material properties and frictional behaviours and additional components such as ligatures and elastic modules, several simplifications were made. The material characteristics and frictional coefficients were chosen based on literature references to accurately reflect the material pairing in the FEA [31]. However, the possible variability of frictional coefficients, particularly in the presence of saliva, was not considered due to the nonlinear behaviour of tribological systems. Depending on the bracket and archwire dimensions, saliva may act as a lubricant or adhesive, affecting bracket-archwire interaction. As observed within investigations on orthodontic sliding mechanics, frictional forces at the bracket-archwire interface during torque expression are considered minimal compared to the primary applied forces [20,31]. While ligatures are commonly used to constrain the archwire within the brackets in the clinical setting, they were not included in the FEA due to the self-ligating properties of the V-bracket which does not require ligatures. Simulating ligatures would have introduced an indefinable bias, due to the different possibilities of ligation and the absence of defined parameters for the simulation process. Clinically, elastic modules ("Alastics") or steel ligatures can be applied. The ligation force of Alastics varies based on several factors, including the degree of pre-stretching during application and the material's properties. Steel ligatures are applied by manual twisting, which produces forces that are difficult to quantify accurately. In summary, ligation forces cannot be consistently or uniformly generated through manual application [32]. Furthermore, the simulations did not account for the behaviour of biological tissues, particularly the periodontal ligament, which plays an essential role in orthodontic tooth movement.

The clinical implications of the present study are limited and primarily indicative regarding the mechanical interactions between bracket and archwire under the defined conditions. However, the findings of the present FEA underline the suitability of V-shaped bracket-archwire configurations made of superelastic NiTi to effectively express torque and prevent both under- and overactivation during torsional loading. Improved torque expression could increase treatment efficiency and accuracy, overcoming a key limitation of current straight-wire orthodontic bracket systems and reducing adverse biological effects such as root resorption. The findings of the study indicate that V-shaped archwires with heights of 0.60 mm and 0.70 mm produce suitable torsional moments at all investigated free path lengths, corresponding to the interbracket distances.

Future research in this field could investigate the behaviour of V-shaped brackets and archwires made from NiTi during orthodontic leveling and sliding or expanding the model to incorporate simulations of biological tissues such as the periodontal ligament and the alveolar bone. Furthermore, experimental and clinical studies are required to confirm the increased accuracy in torque expression using V-mechanics and the suitability of the system in actual orthodontic treatment scenarios.

5. Conclusions

- V-slot brackets in combination with V-shaped archwires made from NiTi exhibited force transmission and moment generation in FEM simulation almost immediately after the onset of the torsional loading
- Both, the transmissible force and torsional moment increased with the torsion angle however in limited amount due to the geometry of the V-shaped archwire interacting with the flexibility of the bracket wings
- The upper torsional moment-limit was found to be around 13–14 Nmm for superelastic V-slot bracket archwire combinations
- Conventional brackets in combination with rectangular archwires made from SS showed torsional losses due to play between the archwire and bracket of about 10–15° depending on the archwire dimension
- With conventional steel brackets, no upper torsional moment limit was present due to the material properties
- In contrast to conventional brackets, both under-activation and over-activation can be avoided using V-slot brackets and V-shape archwires
- V-shaped archwires with heights of 0.60 mm and 0.70 mm produce suitable torsional moments at all investigated free path lengths
- The finite element method proved effective in modeling torque expression for rapid and comprehensive comparison between bracket and archwire materials and geometries.

CRediT authorship contribution statement

Thomas Stocker: Writing – original draft, Software, Methodology, Investigation, Formal analysis, Conceptualization. **Andrea Wichelhaus:** Writing – review & editing, Supervision, Project administration, Conceptualization. **Uwe Baumert:** Validation, Methodology, Data curation. **Mila Janjic Rankovic:** Writing – review & editing, Validation, Data curation. **Corinna Lesley Seidel:** Writing – review & editing, Validation. **Hisham Sabbagh:** Writing – original draft, Supervision, Project administration, Methodology.

Declaration of competing interest

The authors declare the following financial interests/personal relationships which may be considered as potential competing interests:

The author Prof. Dr. Andrea Wichelhaus codeveloped the RED bracket. The RED bracket is manufactured by Redsystem and she is a shareholder of said company.

All other authors declare that they have no potential conflicts of interest.

References

[1] A. Wichelhaus, M. Dulla, H. Sabbagh, U. Baumert, T. Stocker, Stainless steel and NiTi torque archwires and apical root resorption, J. Orofac. Orthop. 82 (2021) 1–12, https://doi.org/10.1007/s00056-020-00244-4.

[2] R.P. Bernisha, G. Mishra, G. Pradeep Raj, P. Chitra, Incisor torque expression characteristics in two passive self-ligating brackets placed at different heights. A finite element investigation, J Oral Biol Craniofac Res 14 (2024) 98–106, https://doi.org/10.1016/j.jobcr.2024.01.003.

[3] Y. Ke, Y. Zhu, M. Zhu, A comparison of treatment effectiveness between clear aligner and fixed appliance therapies, BMC Oral Health 19 (2019) 24, https://doi.org/10.1186/s12903-018-0695-z.

[4] C.A.J. Bauer, M. Scheurer, C. Bourauel, J.P. Kretzer, C.J. Roser, C.J. Lux, L. D. Hodecker, Precision of slot widths and torque transmission of in-office 3D printed brackets : an in vitro study, J. Orofac. Orthop. (2023), https://doi.org/10.1007/s00056-023-00460-8.

[5] A. Wichelhaus, S. Guggenbühl, L. Hötzel, C.L. Seidel, H. Sabbagh, L. Hoffmann, Comparing torque transmission of different bracket systems in combination with various archwires considering play in the bracket slot: an in vitro study, Materials 17 (2024) 684.

[6] L.F. Andrews, The straight-wire appliance, origin, controversy, commentary, J. Clin. Orthod. 10 (1976) 99–114.

[7] M. Tepedino, G. Paiella, M. Iancu Potrubacz, A. Monaco, R. Gatto, C. Chimenti, Dimensional variability of orthodontic slots and archwires: an analysis of torque expression and clinical implications, Prog. Orthod. 21 (2020) 32, https://doi.org/10.1186/s40510-020-00333-5.

[8] R. Gupta, G. Shivaprakash, M.R. Manohar, Sonali. Study model-based evaluation of built-in tip, torque, and in-out characteristics of a third-generation preadjusted edgewise appliance, J. Contemp. Dent. Pract. 19 (2018) 20–29, https://doi.org/10.5005/jp-journals-10024-2206.

[9] B. Zimmer, H. Sino, Coordinating bracket torque and incisor inclination : Part 3: validity of bracket torque values in achieving norm inclinations, J. Orofac. Orthop. 79 (2018) 320–327, https://doi.org/10.1007/s00056-018-0132-6.

[10] A. Wichelhaus, A new elastic slot system and V-wire mechanics, Angle Orthod. 87 (2017) 774–781, https://doi.org/10.2319/121516-899.

[11] T.W. Major, J.P. Carey, D.S. Nobes, P.W. Major, Orthodontic bracket manufacturing tolerances and dimensional differences between select self-ligating

brackets, J. Dent. Biomech. 2010 (2010) 781321, https://doi.org/10.4061/2010/781321, 781321.
[12] A. Arreghini, L. Lombardo, F. Mollica, G. Siciliani, Torque expression capacity of 0.018 and 0.022 bracket slots by changing archwire material and cross section, Prog. Orthod. 15 (2014) 53, https://doi.org/10.1186/s40510-014-0053-x.
[13] A. Archambault, R. Lacoursiere, H. Badawi, P.W. Major, J. Carey, C. Flores-Mir, Torque expression in stainless steel orthodontic brackets. A systematic review, Angle Orthod. 80 (2010) 201–210, https://doi.org/10.2319/080508-352.1.
[14] M. Chung, R.J. Nikolai, K.B. Kim, D.R. Oliver, Third-order torque and self-ligating orthodontic bracket-type effects on sliding friction, Angle Orthod. 79 (2009) 551–557, https://doi.org/10.2319/022608-114.1.
[15] A. Joch, M. Pichelmayer, F. Weiland, Bracket slot and archwire dimensions: manufacturing precision and third order clearance, J. Orthod. 37 (2010) 241–249, https://doi.org/10.1179/14653121043182.
[16] J. Hegele, L. Seitz, C. Claussen, U. Baumert, H. Sabbagh, A. Wichelhaus, Clinical effects with customized brackets and CAD/CAM technology: a prospective controlled study, Prog. Orthod. 22 (2021) 40, https://doi.org/10.1186/s40510-021-00386-0.
[17] L. Hoffmann, H. Sabbagh, A. Wichelhaus, A. Kessler, Bracket transfer accuracy with two different three-dimensional printed transfer trays vs silicone transfer trays, Angle Orthod. 92 (2022) 364–371, https://doi.org/10.2319/040821-283.1.
[18] E.W. Penning, R.H.J. Peerlings, J.D.M. Govers, R.J. Rischen, K. Zinad, E. M. Bronkhorst, K.H. Breuning, A.M. Kuijpers-Jagtman, Orthodontics with customized versus noncustomized appliances: a randomized controlled clinical trial, J. Dent. Res. 96 (2017) 1498–1504, https://doi.org/10.1177/0022034517720913.
[19] N. Alrejaye, R. Pober, R. Giordano II, Torsional strength of computer-aided design/computer-aided manufacturing–fabricated esthetic orthodontic brackets, Angle Orthod. 87 (2016) 125–130, https://doi.org/10.2319/040416-267.1.
[20] R.P. Kusy, P.W. O'Grady, Evaluation of titanium brackets for orthodontic treatment: Part II–The active configuration, Am. J. Orthod. Dentofacial Orthop. 118 (2000) 675–684, https://doi.org/10.1067/mod.2000.97818.
[21] P. Harikrishnan, V. Magesh, A.M. Ajayan, D.K. JebaSingh, Finite element analysis of torque induced orthodontic bracket slot deformation in various bracket-archwire contact assembly, Comput. Methods Progr. Biomed. 197 (2020) 105748, https://doi.org/10.1016/j.cmpb.2020.105748.
[22] D. Allegretti, F. Berti, F. Migliavacca, G. Pennati, L. Petrini, Fatigue assessment of nickel–titanium peripheral stents: comparison of multi-axial fatigue models, Shape Memory and Superelasticity 4 (2018) 186–196, https://doi.org/10.1007/s40830-018-0150-7.
[23] J. Villwock, A. Kinetik Hanau, Dubbel Taschenbuch für den Maschinenbau 1: Grundlagen und Tabellen, 2020.
[24] C.J. Burstone, The segmented arch approach to space closure, Am. J. Orthod. 82 (1982) 361–378, https://doi.org/10.1016/0002-9416(82)90185-3.
[25] H. Gmyrek, C. Bourauel, G. Richter, W. Harzer, Torque capacity of metal and plastic brackets with reference to materials, application, technology and biomechanics, J. Orofac. Orthop. 63 (2002) 113–128, https://doi.org/10.1007/s00056-002-0065-x.
[26] M.A. Casa, R.M. Faltin, K. Faltin, F.G. Sander, V.E. Arana-Chavez, Root resorptions in upper first premolars after application of continuous torque moment. Intra-individual study, J. Orofac. Orthop. 62 (2001) 285–295, https://doi.org/10.1007/pl00001936.
[27] Y.A. Yassir, G.T. McIntyre, D.R. Bearn, Orthodontic treatment and root resorption: an overview of systematic reviews, Eur. J. Orthod. 43 (2021) 442–456, https://doi.org/10.1093/ejo/cjaa058.
[28] A. Wichelhaus, T. Eichenberg, P. Gruber, E.P. Bamidis, T. Stocker, Friction force adjustment by an innovative covering system applied with superelastic NiTi brackets and wires-an in-vitro study, Materials 15 (2022), https://doi.org/10.3390/ma15124248.
[29] T.R. Meling, J. Odegaard, D. Seqner, On bracket slot height: a methodologic study, Am. J. Orthod. Dentofacial Orthop. 113 (1998) 387–393, https://doi.org/10.1016/s0889-5406(98)80009-7.
[30] DIN. 13996:2012-08; Dentistry-Dimensions for Archwires and Attachments for Orthodontic Appliances, 2012, https://doi.org/10.31030/1888741.
[31] R.P. Kusy, J.Q. Whitley, Friction between different wire-bracket configurations and materials, Semin. Orthod. 3 (3) (1997) 166–177.
[32] L.R. Iwasaki, et al., Clinical ligation forces and intraoral friction during sliding on a stainless steel archwire, Am. J. Orthod. Dentofacial Orthop. 123 (4) (2003) 408–415.